CHAPTER III
PREPARATION AND CHARACTERIZATION OF NANO ZERO-VALENT IRON COATED ON DIATOMITE

This experimental study is divided into two sections. In the first section, it explains the synthesis methodology of nano zero-valent ions coated on diatomite and the characterization techniques of adsorbent. Finally, the result of comparison of adsorbent performances were reported.

3.1 Experimental

3.1.1 Chemicals and materials

Diatomite powder of 150 micron was achieved from the North Thailand. All chemicals using in all the experiments were obtained in analytical-grade reagents; namely, iron (III) sulphate ($FeSO_4.7H_2O$, Ajax Finechem; Australia), sodium borohydride ($NaBH_4$, Rankem; India), potassium bromide (KBr, Sigma-Aldrich; UK) ,ammonium hydroxide (NH_4OH, Panreac; Barcelona) and hydrogen chloride (HCl_2, RCL Labscan; Thailand). A distilled water purified with a illipore Milli-Q equipment (resistivity of 18 MV cm) was used in all the experiments.

3.1.2 Preparation of nZVI-D

In the present study, there were two sections of preparation of nano zero-valent ion coated on diatomite (nZVI-D). In the first section, diatomite, used to support nano zero-valent ion particles, was soaked in distilled water for 12 h. Next, synthesize iron-oxide-coated diatomite (IOCD) was prepared by the method similar to the method used by Pan et al. (2010) (Pan, Chiou, & Lin, 2010) for coating iron oxide onto diatomite. Then, about 10 g of diatomite was mixed with 27.80 g of $FeSO_4.7H_2O$ in distilled water (100 ml) and stirred for 1 h. The soaked diatomite was dried at 110°C. After drying, a solid was washed with deionized water until the solution was cleared and dried in an oven for 24 h. After that, the IOCD particles were stored in a desiccator. In another section, about 1 g of IOCD was reduced by freshly prepared

sodium borohydride ($NaBH_4$) solution (0.946 g of $NaBH_4$ in 50 ml). After that, the $NaBH_4$ solution was added drop into the solution and constantly stirred for 30 min. In this step, nano zero-vatent iron (nZVI) particles immediately appeared after the first drop. The synthetic reaction occurred as the following reaction:

$$2Fe^{2+} + 4BH_4^- + 2H_2O \rightarrow 2Fe^0 + 4BO_2^- + 2H_2 + 4H^+ \quad (3.1)$$

Finally, nZVI-D were collected and washed thrice with ethanol to prevent oxidation. The prepared nZVI-D samples are identified as nZVI-D_N, where N denotes the number of iron oxide coating times (single to tripple). To conclude, nZVI-D can be prepared by the reduction of ferrous ion and diatomite with $NaBH_4$.

3.1.3 Characterization of nZVI-D

A X-ray fluorescence (XRF) analysis was carried out to determine chemical compositions of nZVI-D and diatomite. The nZVI-D surface area was measured by a Burnauer-Emmrtt-Teller (BET) theory and a nitrogen adsorption method at 77 K on the ASAP 2010 analyzer (Micromerition, USA). The surface morphology was characterized by a scanning electron microscope (SEM, S-3000N, Hitachi, Japan) and a transmission electron microscope (TEM, FEI/TECNAI G2 20, USA). The TEM samples were prepared by drop of the nano-particle suspension onto a lacey carbon film which was supported by a copper TEM grid. The chemical composition and the crystallographic structure were determined by X-ray diffraction (XRD, Bruker D8 Advance; Germany) with CuαK radiation (40 kV, 40 mA). X-ray diffraction patterns of nZVI-D over a wide range of angles (10-80°, 2θ) were measured. Fourier transform infrared spectroscopy (FTIR, Bruker Tensor 27, USA) was used to determine the amount of components in a mixture and interfacial bonding mechanism of silica and iron. The sample mixed in KBr pellet at room temperature, spectra were gotten over the range of 400-4,000 cm^{-1}. The point of zero charge (pH_{pzc}) was determined by Zetasizer Nano Z (Malvern Instruments Ltd., UK). Measuring the ζ-potential in the range pH 1-12 and the solution pH was adjusted by adding 1 N HCl or 1 N NaOH. It is a concept relating to the phenomenon of adsorption, and describes the condition when the electrical charge density on a surface is zero. Then, X-ray

Absorption Near Edge Structure (XANES) was carried out on beamline 2.2 and 8 of Synchrotron Light Research Institute (Public Organization), Thailand.

The valence elements and distinction between different oxidation states of elements in nZVI-D before and after adsorption lead ion within a depth of <10 nm was obtained on An X-ray photoelectron spectroscope (XPS, AXIS Ultra DLD, UK). The survey and multiregional spectra were recorded of Pb 4f, O 1s, Fe 2p3/2, Fe 2p1/2, Si 2p and Al 2p.

3.1.4 Comparison study of adsorbent performances

To compare the practical removal performance, nZVI-D (1 g), nZVI (0.085 g), diatomite (1 g) and SiO_2 (1 g) were applied in As^{5+} removal. The batch experiments were conducted in duplicate using a conical flask containing 1000 mL 1,000 µg/L solution at 30°C with initial pH value of 4.0. The mixture in the reactor was stirred with the speed of 160 rpm for 60 min. The samples were taken at certain time intervals, and analyzed immediately after being filtered through a 0.45 µm filter membrane. The initial and final As^{5+}concentrations of the solutions were measured with a hydride atomic absorption spectrophotometer (HD-AAS, Perkin Elmer series Analyst 880, UK). The percentages of As^{5+} removal, (% As^{5+} removal) were calculated as follows:

$$Y = \frac{C_0 - C_t}{C_0} \times 100 \tag{2.20}$$

where, C_0 is the initial concentration of As^{5+} (mg/L) and C_t is the concentration of As^{5+} (mg/L) after adsorption at time. Y is the percentage As^{5+} removal.

3.2 Results and discussion

3.2.1 Characteristics of adsorbent

The XRF data of the raw diatomite suggests that it consists of SiO_2 (79.761%), Al_2O_3 (9.618%), FeO (2.496%), MgO (0.853%), K_2O (0.746%), CaO (0.160%), and TiO_2 (0.147%). The XRD pattern of diatomite and nZVI-D_N are presented in Fig. 3.1., The diffraction spectrogram indicates that the diatomite consists mainly of silica (SiO_2) white silica phase proves quartz and tridymite,

respectively (Köseoglu, Köksal, Çiftci, & Akkurt, 2005). The increased amounts of iron oxide in resulted in nZVI-D_N decreasing the major peak intensity of quartz band. This is the increase of iron oxide on the several coatings resuting that the pore structure of diatomite was blocked and iron oxide silts overspread on the surface of diatomite.

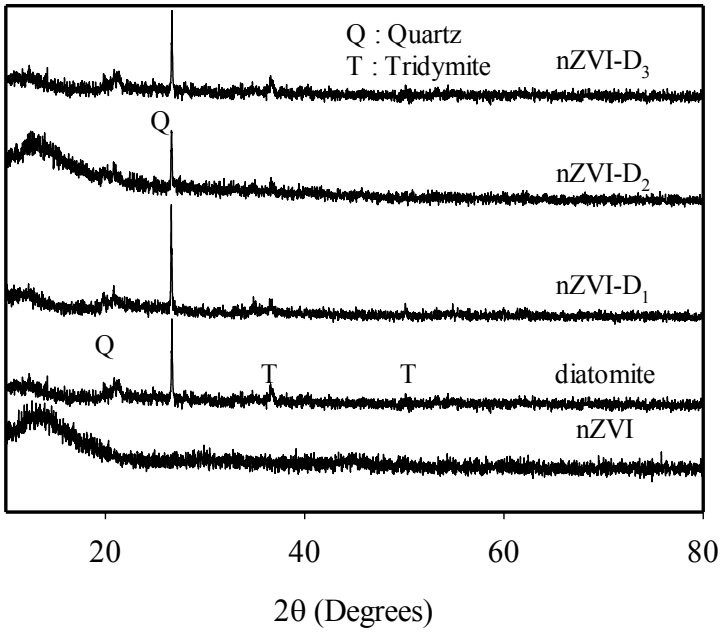

Figure 3.1 XRD patterns of diatomite, nZVI, nZVI-D_1: single iron oxide coating, nZVI-D_2: double iron oxide coating and nZVI-D_3: tripple iron oxide coating

Determination quantity of Fe oxide in diatomite was done by digesting metal of adsorbents of 1 g and deionized water of 200 mL and nitric acid of 5 mL, and then heating it up until the solution volume remained about 20 mL which the results are similar to results of XRF. Subsequently, the measurement of Fe oxide amount on the adsorbent in the solution was carried out by atomic absorption spectroscopy. The AAS results showed that the dosage of Fe oxide in diatomite in single iron oxide coating was 2.87% by weight, double iron oxide coating was equal to 8.59%, and tripple iron oxide coating increased to 9.30%, which is similar to Wantala et al. (2012). It interesting notes that the double iron oxide coating has the amount of Fe oxide of is greater than the single iron oxide coating to 0.057 g. Due to the Fe oxide

inserted into the porous of diatomite and the amount of Fe oxide load into the surface of diatomite more than the single iron oxide coating. However, the amount of Fe oxide in the tripple iron oxide coating was slightly increased, less than 10 %, from the double iron oxide coating. It is my belief that the Fe oxide was fully insert into the porous structure of the diatomite and accrued on the outer surface which the results supported by the SEM images.

The surface areas of adsorbents were calulated using the BET equation which found that the surface area of diatomite and nZVI was 26.80 and 24.06 m^2/g, respectively, however the surface area of nZVI-D_1 was decreased to 17.69 m^2/g and the total pore volume was decreased from 0.069 to 0.052 cm^3/g. In the same way, the surface area of nZVI-D_2 was reduced to 14.16 m^2/g, which was less than nZVI-D_1 because the amount of nZVI on diatomite has more volume which resulting that the total pore volume was decreased to 0.050 cm^3/g. The results of surface area were consistent with the results of the amount of Fe oxide above and similar to the work of Zhu et al. (Zhu, Jia, Wu, & Wang, 2009). When it has more amounted of Fe oxide as a result the surface area deceased because iron oxide blocked the pore structure of diatomite in the cause of nZVI-D_1 and nZVI-D_2. In contrast, the surface area and the total pore volume of nZVI-D_3 increased to 33.35 m^2/g and 0.075 cm^3/g, respectively while the amount of Fe oxide rose. Due to, the structure of diatomite fractured of excessive amounts of iron oxide which was consistent with the results of SEM as depicted in Fig. 3.2 (b-d). It saw from SEM micrographs found that the amount of iron oxide blocked the porous structure of diatomite for the single to the double iron oxide coating and the iron oxide dispersed well in surface of diatomite. In the tripple iron oxide coating, the structure of diatomite was broken to pieces and was covered by iron oxide. Whereas, the surface morphology of a diatomite pure was composed of plaque and circular-shape diatom particles with sizes of 0.005–0.025 mm in clay matrix (Caliskan, Kul, Alkan, Sogut, & Alacabey, 2011) shown in SEM images (Fig. 3.2a).

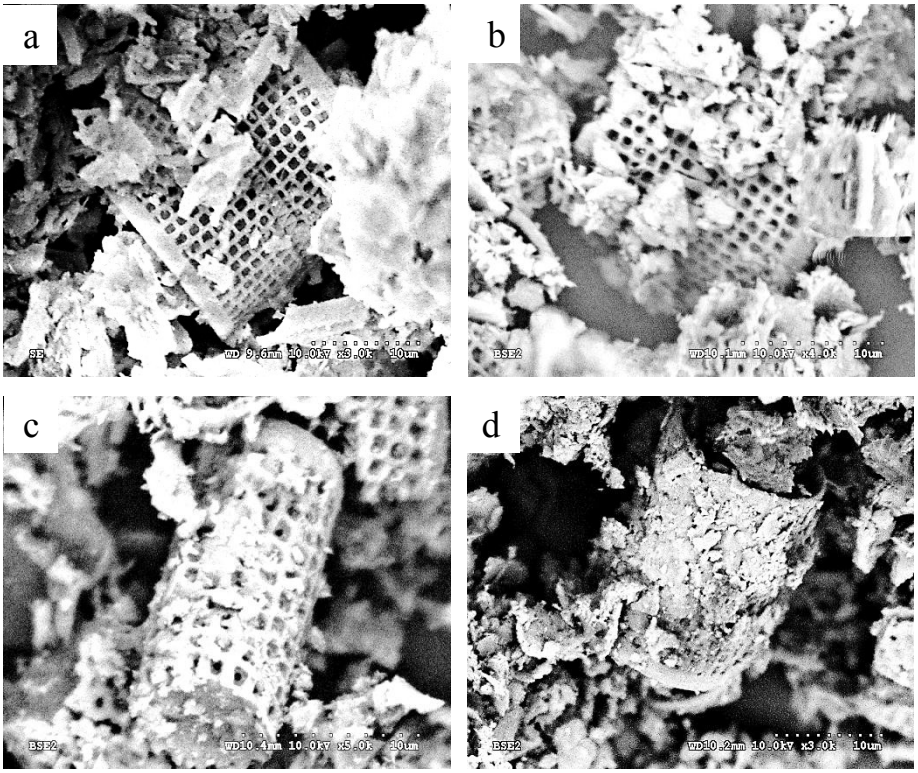

Figure 3.2 Scanning electron microphotograph of (a) diatomite (b) nZVI-D_1 (c) nZVI-D_2 and (d) nZVI-D_3

Fig. 3.3a displays TEM images of a nZVI formations which appear a chainlike of spherical nanoparticles and aggregated structure because of magnetic interactions, electrostatic interactions, and Van der Waals force between the nanoparticles and a natural tendency to remain in more thermodynamically stable state (Kim et al., 2013; Ryu, Jeong, Jang, & Choi, 2011; Yun, Cho, Jang, & Park, 2013). The particles of nZVI displaied clear core-shell structure consisting of black core and brighter shell layer. Practically, black core assumed as Fe^0 and brighter shell as oxide shell layer of iron oxides and iron hydroxide shown in Fig. 3.3a expansion. Therefore, an oxidized layer was illustrated with contact to oxidizing agents, mainly dissolved oxygen (Woo et al., 2014; Zhu et al., 2013). In contrast, nZVI-D_2 (Fig. 3.3b) shows roughly spherical of nZVI particles, well separate and dispersed of nZVI particles in surface of diatomite. This indicated that the presence of diatomite as support and protected nZVI from agglomeration and made nZVI to have short chains and small agglomerates as well as the research of Zhang, Jiang, Zhang and Xie

(Zhang, Jiang, Zhang, & Xie, 2013). However, the particle diameter of nZVI pure and nZVI coat on diatomite were equal mainly 50-70 nm. In sum up, the combination with nZVI and diatomite in this research was a great choice against nanoparticle aggregation.

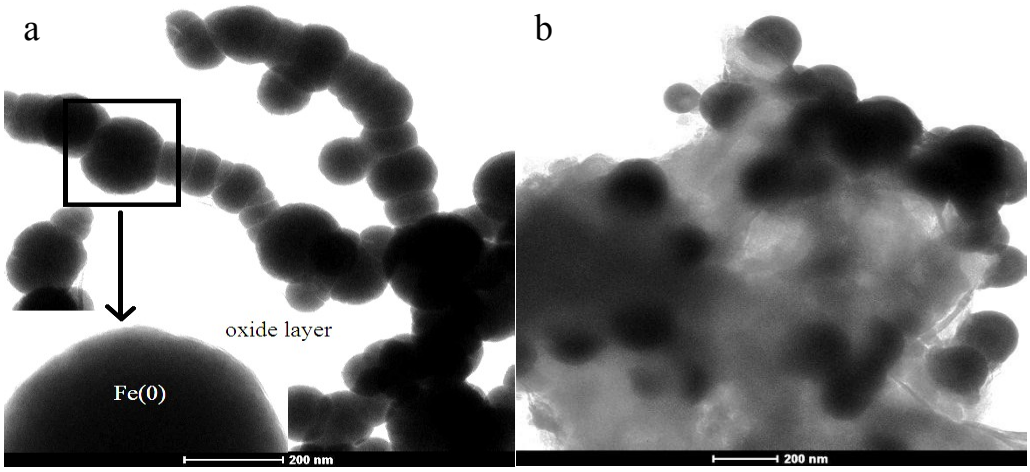

Figure 3.3 TEM images of (a) nZVI particles and
(b) nZVI supported on diatomite (nZVI-D_2)

Fig. 3.4 shows the FT-IR spectrums of diatomite had shown the major adsorption bands at 3,695, 1,029, 796, 693, 551 and 412 cm^{-1}. The band at 3,695 cm^{-1} was the free silanol group (SiO-H) on the surface. The peaks at 1,029 and 412 cm^{-1} were ascribed to the asymmetric stretching modes of Si-O-Si bonds, and the peak at 796 cm^{-1} was correspond to SiO-H vibration (Caliskan, Kul, Alkan, Sogut, & Alacabey, 2011; Zhang, Lin, Chen, Megharaj, & Naidu, 2011). Moreover, The FT-IR spectra of iron oxide coat diatomite showed the new adsorption peaks at 550 and 437 cm^{-1} corresponding to Fe-O stretches of Fe_2O_3 and Fe_3O_4, and the peak at 595 cm^{-1} may correspond to Fe-O stretches of Fe-O-Si and δ-FeOOH which could be confirmed by the peak at 447 cm^{-1} (Hu, Lo, & Chen, 2007). The peak of Fe_2O_3, Fe_3O_4 and δ-FeOOH indicated that reduction with $NaBH_4$ to nZVI-D_N could easily happen since the binding bond of iron oxide on the diatomite was not strong, so $NaBH_4$ can be reactive easily.

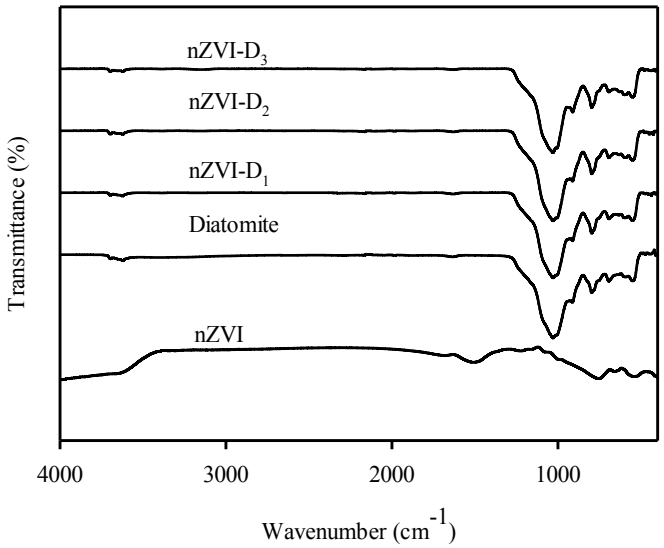

Figure 3.4 Fourier transforms infrared spectroscopy of (a) diatomite (b) nZVI-D_1 (c) nZVI-D_2 and (d) nZVI-D_3

The XPS spectra of nZVI-D_2 directed also the existence of Fe 2p 709.1 eV, O 1s 530.1 eV, C 1s 283.1 eV, Si 2p 101.1 eV and Al 2p 73.1 eV as indicated in Fig 7a. The peaks at 705.3 eV correspond to zero-valent iron (Fe^0 $2p_{3/2}$), while 711.5 eV and 725.2 eV relate to Fe $2p_{3/2}$ and Fe $2p_{1/2}$ binding energies. The main iron species of nZVI-D_2 were Fe^0, Fe_2O_3 ,$Fe(OH)_3$ and FeOOH (Hermas, 2008) displaied in Fig 3.5b. It confirmed that the core shell structure of nZVI-D present iron oxides and iron hydroxide consistent with research of X. Zhang (Zhang et al., 2011). Through the binding energy analyzes, the Al 2p peak at 73.4 eV and 74.6 eV were AlOOH and $Al(OH)_3$ respectively, while Si 2p peaks at 101.7 eV and 102.8 eV were assigned to the Si-O and Si-OH, respectively shown in Fig 3.5c-d,

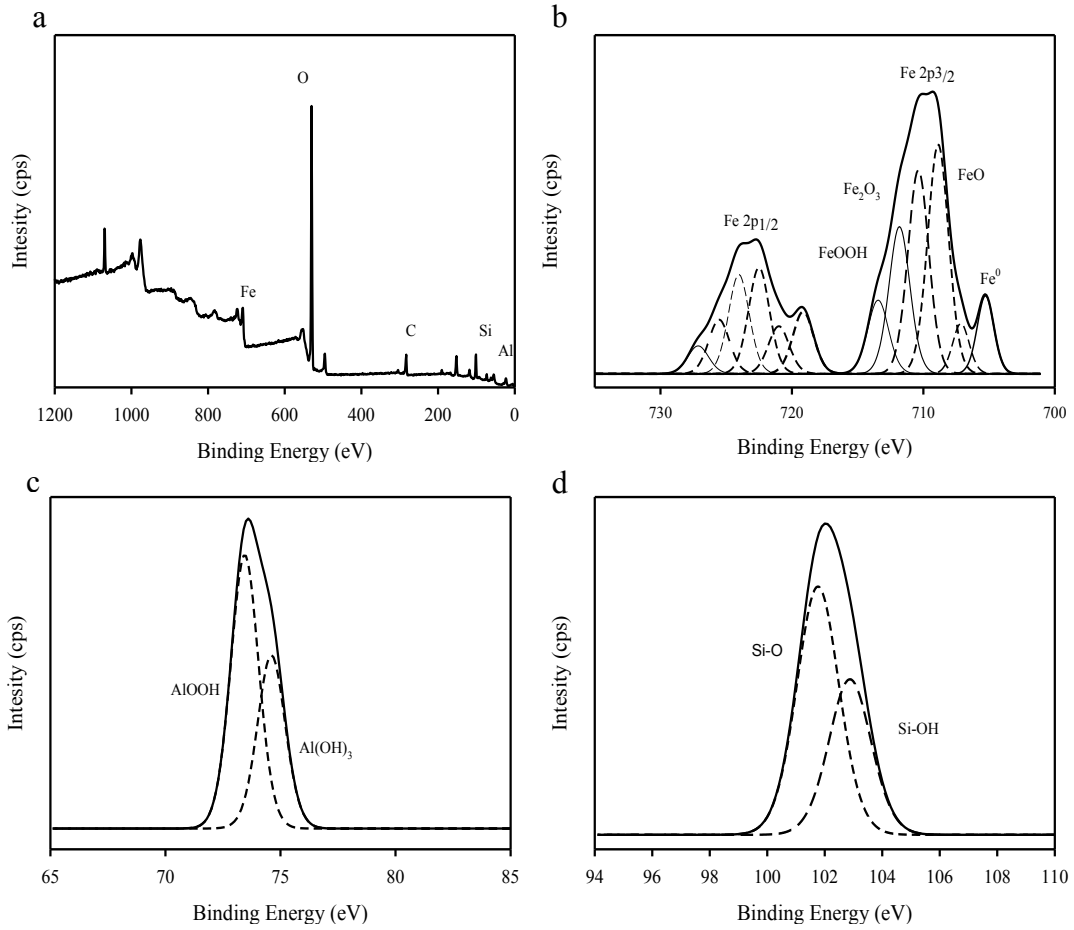

Figure 3.5 XPS spectra of (a) full survey of nZVI-D_2
(b) Fe (c) Si and (d) Al in nZVI-D_2

Fig. 3.6 shows zero point of charge (pH_{pzc}) of diatomite, nZVI and nZVI-D, where the diatomite and nZVI-D carried a lower pH_{pzc} than nZVI. The pH_{pzc} of nZVI (pH 6.4) is close to that of pristine nZVI (pH 7.7) as reported by Kanel et al. (Kanel, Manning, Charlet, & Choi, 2005). However, after modified nZVI with diatomite, the pH_{pzc} of nZVI-D has been shifted to pH 2 because nZVI-D has amount of nZVI equal only to 8.6% on diatomite. The pH_{pzc} has affected on heavy metal adsorption, that is, pH of solution greater than pH_{pzc}, the adsorbent surface is negative. The pH of solution is equal to pH_{pzc}, the surface charge of adsorbents is neutral. At pH values lower than pH_{pzc}, the adsorbent surface becomes positively charged (Al-Ghouti, Khraisheh, Ahmad, & Allen, 2009).

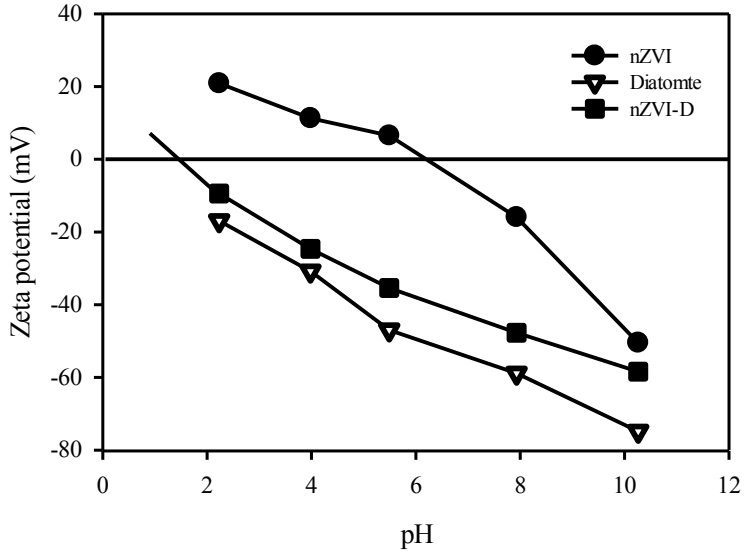

Figure 3.6 Zeta potential charge of nZVI, Diatomite and nZVI-D as a pH function

3.2.2 Comparison study of adsorbent performances

In this work, nZVI, nZVI-D, SiO_2, and diatomite were used as adsorbent for removing As^{5+} from aqueous solution in a batch system. The adsorption efficiencies are shown in Fig. 3.7. The results of As^{5+} adsorption showed that the nZVI-D was the best effective adsorbent. The present of zero-valence iron in the nZVI-D enhanced the higher adsorption of As^{5+} than diatomite pure only. It has been found that the equilibrium time taken very fast in 3 min. The nZVI had removal efficiency lower than the nZVI-D when used to remove As^{5+} in 10 min. The best removal efficiency of the nZVI-D may have been caused by the aggregation of the nZVI decreasing its specific surface area and reaction activity (Arshadi, Soleymanzadeh, Salvacion, & SalimiVahid, 2014). The diatomite supported nZVI was a stable material and dispersed the nZVI in aqueous solution increasing the activity of the nZVI.

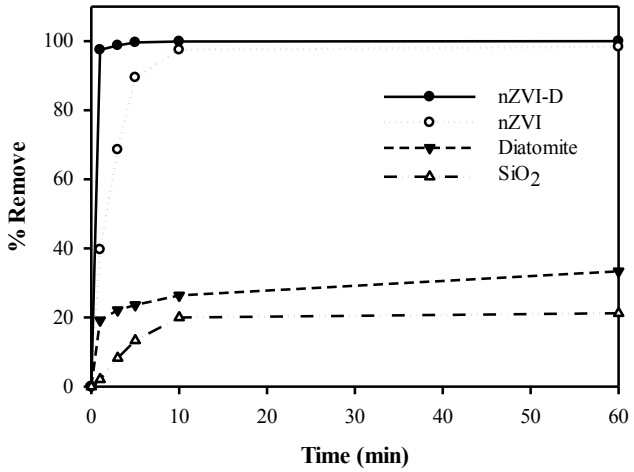

Figure 3.7 Effects of adsorbent type on As^{5+} adsorption, at 30±5 ºC, 1,000 µg/L, pH 4 and 0.085 g of nZVI, 1 g of nZVI-D, diatomite and SiO_2.

3.3 Conclusions

A composite of nano zero-valent iron coated on diatomite (nZVI-D) has been modern synthesized which was prepared by impregnation of diatomite with iron sulphate solution, and followed by reducing with sodium borohydride. The second-round of coating has the most efficiently because it suitable of surface area, pore structure, which the iron oxide has good dispersion on the surface of diatomite. The results obtained from SEM showed that nZVI coated on diatomite was well dispersed and helped to decrease aggregation. The XPS spectra display Fe^0, Fe_2O_3, $Fe(OH)_3$ and FeOOH in the adsorbent. The study of adsorbent performances was found that the nZVI-D exhibited the best effectiveness in the removal of As^{5+} from aqueous solutions. Thus, the achieved results indicate that the nZVI-D adsorbent is a potential media for As^{5+} removal from watewater.

3.4 List of abbreviations

Y	percentages As^{5+} removal
C_0	initial concentration (mg/L)
C_i	remaining concentration at any time (mg/L)